Technical Paper
Int'l J. of Aeronautical & Space Sci. 12(4), 385–395 (2011)
DOI:10.5139/IJASS.2011.12.4.385

IJASS
International Journal of Aeronautical and Space Sciences

Monte Carlo Simulation on Reliability of a Self-Separable Ejector for Man-Portable Missiles

Hyo-Nam Lee* and Jong-Yun Oh**

Rocket Propulsion Directorate, Agency for Defense Development, Daejon 305-600, Korea

Abstract

An ejector was developed for man-portable missiles. The ejector can be separated from the missile after the completion of the ejection function even without any additional separation devices. This paper introduces the particular separation mechanism of the ejector and presents the methodology, based on a probabilistic design method, to predict the ejection-and-separation reliability. This approach using Monte Carlo simulation can also be applicable to the reliability prediction of one-shot items suffering from difficulties in estimating or in demonstrating their reliability due to the lack of the number of tests available.

Key words: Monte Carlo simulation, Reliability, Ejection, Separation

Nomenclature

A_b	=	propellant burning area
$A_{cylinder}$	=	area of the separation cylinder
A_e	=	nozzle exit area
A_{pin}	=	cross sectional area of fastening pins
A_t	=	nozzle throat area
a	=	burning rate constant
B	=	stress variable
C	=	strength variable
C_D	=	discharge coefficient
C_F	=	thrust coefficient
C_p	=	specific heat at constant pressure
C_v	=	specific heat at constant volume
D; D_1, D_2	=	failure variable; for failure mode 1, for failure mode 2
$\bar{D}$	=	mean of failure variable
e	=	burning distance
F_1	=	thrust of ejector
F_2	=	force generated by the separation cylinder
F_{pin}	=	force required to shear fastening pins
M_w	=	molecular weight
m	=	missile weight
$\dot{m}$;$\dot{m}_{gen}$, $\dot{m}_{10}$, $\dot{m}_{12}$	=	mass flow rate; for generation, from chamber to atmosphere, from chamber to cylinder

* Principal Researcher, Corresponding author, E-mail : lhn4577@add.re.kr.
** Principal Researcher, Rocket Propulsion Directorate, jyo4526@add.re.kr.

Received: August 19, 2011 Accepted: December 07, 2011

http://ijass.or.kr pISSN: 2093-6742 eISSN: 2093-2480

n	=	burning rate exponent
P; P_1, P_2	=	pressure; for the burning chamber, for the separation cylinder
P_a	=	ambient pressure
P_e	=	pressure at nozzle exit
Q	=	unreliability
$\dot{Q}_{loss}$	=	heat loss of cylinder
R; R_1, R_2	=	reliability; for failure mode 1, for failure mode 2
R_g	=	gas constant
r_b	=	burning rate
s_D	=	standard deviation of failure variable
T; T_1, T_2	=	temperature; for the burning chamber, for the separation cylinder
T_f	=	flame temperature
t_{min}	=	time that separation must not occur
t_{max}	=	time that separation must occur
U	=	variable represents minimum limit in Eq. (5)
V	=	variable represents shearing of fastening pins in Eq. (5)
V_1	=	volume of the burning chamber
V_2	=	volume of the separation cylinder
v	=	ejection velocity
v_R	=	required ejection velocity
W	=	variable represents maximum limit in Eq. (5)
Z	=	standard normal deviate
Z_0	=	lower integration limit in Eq. (4)
α	=	half angle of nozzle divergence cone
γ	=	specific heat ratio
ΔF	=	force difference
ρ; ρ_1, ρ_2	=	gas density; for the burning chamber, for the separation cylinder
ρ_p	=	propellant density
σ_{shear}	=	shear strength of pin material
φ	=	probability density function of standard normal distribution
Φ	=	cumulative distribution function of standard normal distribution

1. Introduction

The main rocket motor used in man-portable missiles must be ignited at a sufficient distance from the gunner due to the danger of its exhaust plume. Some devices are thus needed for ejecting the missile from the launch tube with a certain velocity. For this purpose, an additional small rocket motor (hereafter called "ejector") having a very short burn time of less than about 0.1 second is generally employed. Once the missile is ejected, the ejector is preferably separated from the missile since no further function is to be performed and unnecessary weight acts against flight performance. Hence, the separation of a post-fired ejector has been a trend in highly maneuverable man-portable missiles. For the ejector separation, additional devices such as pyrotechnic actuated devices are widely used. As shown in Fig. 1, however, we have designed an ejector that can be separated from the missile without help of any additional devices.

The ejector must satisfy two requirements: a sufficient ejection velocity and a highly reliable separation. The ejector must expel the missile from the launch tube with a required velocity since a low ejection velocity can cause either the loss of the flight altitude of the missile or harm to the gunner due to main motor ignition at a too close distance. Meanwhile, the ejector must be separated from the missile after functioning since the onset of the next event of the missile is usually determined by whether or not the separation succeeds. If the separation fails, the next sequence such as the main motor ignition no longer proceeds because of safety, which results in the total mission failure of the missile. In this respect, the reliability on the ejection-and-separation of the aforementioned ejector has been a subject of practical

importance.

Reliability can be defined as numbers representing the probability that an item will function without failure. In general, mechanical devices or electrical components can be assembled into the system after confirming their reliabilities by a test. In other words, those items can be repeatedly tested until the sufficient reliability data are obtained. On the other hand, it is impossible to confirm the functions for one-shot items such as the ejector prior to the use of actual situations because those items become useless once they are fired for the test. For this reason, the reliability estimation of this type of item has depended significantly on the number of firing tests available in a conventional method. For example, at least 10,000 items are needed for 99.99% reliability.

This conventional approach, based on a large number of firing tests with full scale items, would require considerable time and cost to achieve statistically significant reliability (Perkins and Fragola, 1989; Wood, 1983; Zhang and Shiue, 2001). Moreover, problems found during a test are very difficult to correct in terms of the schedule because firing tests are usually performed at the end of the development phase. Indeed, if the item were to be modified after many tests were conducted for calculating reliability, the accumulated data could become useless in reliability calculation since this approach is based on the assumption that all of the test items are the same. Due to these difficulties this type of item has long been used without confidence of whether it functions well. Further, so far no report has been made of any related research attempt to represent the reliability of the items. We will address the possibility of such research in the present work.

An alternative approach is available, based on a probabilistic design concept. The method not only provides the ability to estimate reliability without numerous firing tests but also can be applicable to all program phases. This approach regards all the variables included in the design, fabrication, and operation of the items as random variables having their own probability distributions instead of point values. We employ this probabilistic approach to overcome the long-standing troublesome problem of representing the reliability for the items. The objective of the present work was two-fold: (1) to introduce a particular separation mechanism of the newly devised self-separable ejector and (2) to present a methodology based on the probabilistic design method known as a stress-strength model for predicting the reliability of the ejector. Particular subjects of interest were what reliability value is and which variables dominantly affect reliability. For this purpose, Monte Carlo (MC) simulation is employed. The current approach can, in general, be extended to various other one-shot items.

2. Ejector

2.1 Ejector configuration

Figure 1 is a schematic of the ejector. The ejector has the same configuration with a typical rocket motor, consisting of the igniter, propellant charge, combustion chamber, and nozzle, except for the separation cylinder which is assembled between the missile and the combustion chamber having orifices. The ejector is fixed at the aft end of the missile by fastening pins. Here, we designate the combustion chamber as 1 and the separation cylinder as 2.

The thrust F_1 is generated in proportion to the nozzle throat area and the gas pressure P_1 which is generated by burning propellant in space 1 with volume V_1. This thrust is utilized for ejecting the missile from the launch tube. Some of the combustion gas generated in space 1 can flow into space 2 with volume V_2 through the orifices. Also, the force F_2 is gradually generated and is proportional to the area of the separation cylinder and the gas pressure P_2 by inflowing gas.. F_1 and F_2 are opposite to each other in direction. The four major parameters of P_1, P_2, F_1, and F_2 could be varied with time as shown in Fig. 2, and were dependent on many design variables including the burning area of propellant charge, burning rate of propellant, size of nozzles, orifice size, area of the separation cylinder, and so on. The fastening pins fixing the missile and the ejector are cut by the interaction of F_1 and F_2, which results in the separation.

2.2 Separation mechanism

A specific feature of the ejector is that a premature separation should be avoided. In the present work, the premature separation can be defined as the case when the

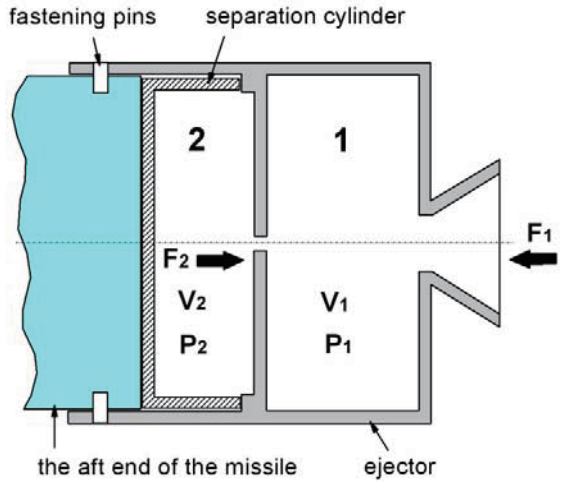

Fig. 1. Schematic of the newly devised ejector.

separation occurs even though the missile does not reach the required level of ejection velocity. If the separation occurs when the propellant of the ejector is still burning, the leftover impulse can no longer be utilized to thrust the missile because the contact between the missile and the ejector is broken. The required ejection velocity is preferably achieved by using the minimum amount of propellant since excessive propellant can incur detrimental effects in terms of a large back-blast and a high chamber pressure. This can be interpreted to mean that the separation should occur near the point of the completion of web burn. This requirement can be met by the following separation mechanism.

F_1, assigned a minus sign, cannot act as the cutting of the fastening pins because the force was transmitted to the missile through the separation cylinder, not the pins; whereas F_2, assigned a plus sign, can be exerted to cut off the pins. Because F_2 is offset by F_1 with the opposing direction, however, the force for cutting the pins can be developed only in a condition whereby F_2 is larger than F_1; that is, only when the difference of the two forces, $\Delta F = F_2 - F_1$, is positive. As shown in Fig. 3, the force difference varies with time. The cutting force did not exist since $\Delta F<0$ before reaching the point of "b" where $\Delta F=0$. Subsequently, the force difference continuously increased until the point of "d", which is the point of web-burn completion, then rose sharply to the peak and then gradually decreased in the final stage. The drastic increase beyond the point of "d" occurs because F_1 is more rapidly decreased than F_2. This was attributed to the fact that P_1 decreases very fast at the burn out of propellant whereas P_2 decreases relatively slowly because the combustion gases flow out through the small orifices. A time point in which the pins are cut can be controlled by the shearing force of the pins, F_{pin}. If the cutting force is greater than the shearing force of the pins, i.e., $\Delta F \geq F_{pin}$, the pins can be cut off and the ejector separation will occur.

The separation must occur between t_{min} and t_{max} as represented in Fig. 3. t_{min} is the lower time limit at which the separation must not occur. This limit can be determined by the impulse, which is the shaded area in Fig. 3, corresponding to the ejection velocity of $v = \frac{1}{m}\int_0^{t_{min}} F_1 dt$. The pins must not be severed before this limit is reached. It is preferable for t_{min} to be as close as possible to the web burn time. Meanwhile, t_{max} is the upper time limit at which the separation must occur, which corresponds to the maximum cutting force. The pins must be cut off before the reach of this limit.

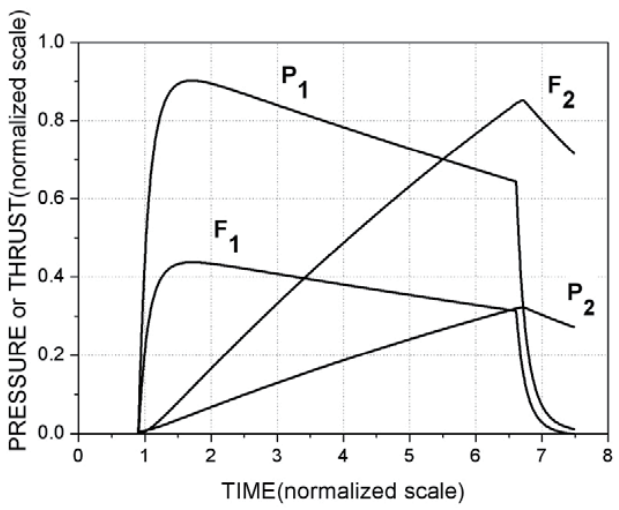

Fig. 2. Relationship among four major parameters determining the function of the ejector (the scales were normalized by arbitrary numbers).

3. Simulation Methodology for Reliability Prediction

3.1 Definition of failure modes

Many failure modes are possible in the function of the ejector, such as ignition failure, structural failure, overpressure, and too long burn time. However, only the

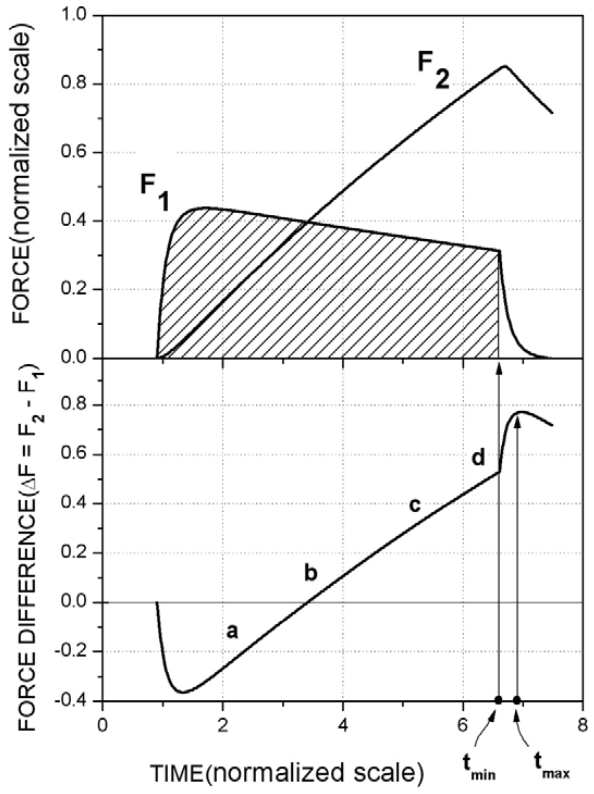

Fig. 3. Time-dependent variation of the forces for the separation.

DOI:10.5139/IJASS.2011.12.4.385

following two failure modes will be considered in this paper:

1) Failure mode 1: no separation of the ejector

2) Failure mode 2: insufficient ejection velocity

Failure mode 1 occurs when the pins are not cut off; whereas failure mode 2 occurs when the premature separation occurs. Two assumptions were made. Firstly, the reliability values of all the failure modes involved in all of the components of the ejector are all one, except for the two failure modes mentioned above. Secondly, all of the failure modes are independent of each other. The overall reliability (R_t) can thus be regarded as the product of the reliability of failure mode 1 (R_1) and the reliability of failure mode 2 (R_2).

3.2 Probabilistic design method

The failure modes of a one-shot item such as the ejector are normally characterized by a 'static failure.' In other words, when the item is operated or tested, there can be only two possible outcomes: a success or a failure. This nature of the static failure enables us to apply the probabilistic design method to reliability prediction. The most common type of model used to describe the static failure is known as the stress-strength model (Johnson, 1988; Kececioglu, 2003). According to this model, the failure function or failure variable, D, can then be simply defined as follows:

$$D = C - B \tag{1}$$

where C is "strength" as measured on an applicable scale and B is "stress" as measured on the same scale. The variable D is the difference between C and B. In this model, both C and B are not point values but random variables with their own probability density functions (*pdf*) as shown in Fig. 4.

If the stress exceeds the strength, i.e., B>C, failure may occur. Therefore, the overlapped region, shaded in Fig. 4, of the two distributions implies the unreliability, Q, as follows:

$$Q = \Pr(B > C) = \Pr(D \le 0) \tag{2}$$

Since '1-Q' gives the reliability, the reliability R is given by all the probabilities whereby the strength exceeds the stress or D is greater than zero. Therefore, R can be calculated by the integration of the *pdf* of D, f(D), from zero to infinity as follows:

$$R = 1 - Q = \Pr(B < C) = \Pr(D > 0) = \int_0^\infty f(D)dD \tag{3}$$

If the variables of C and B are independent and normally distributed, the probability density D can also be assumed as normally distributed with its mean value $\overline{D}$ and the standard deviation s_D. Under this assumption, the R of Eq. (3) can be simply evaluated using probability information of the standard normal distribution as shown below:

$$R = \int_{Z_0}^{\infty} \phi(Z)dZ = 1 - \Phi(Z_0) = \Phi(-Z_0) \tag{4}$$

where Z is a standardized variable of D and $Z_0 = -\frac{\overline{D}}{s_D}$ is the lower integration limit.

3.3 Simulation model

To predict reliability of two failure modes, a simulation model based on the probabilistic design method was proposed. In the simulation model, the three major variables of t_{min}, t_{max}, and F_{pin} were considered, which affect the ejector's function. The two limits of t_{min} and t_{max} were converted into U and W, respectively, to have the same unit with the force F_{pin} as given in Fig. 5 and Eq. (5).

$$\begin{cases} U = \min\limits_{v \ge v_R} \{F_2 - F_1\} \\ V = F_{\mathbf{pin}} \\ W = \max\{F_2 - F_1\} \end{cases} \tag{5}$$

This expression helps us to make a model based on the probabilistic design method. In the above equation,

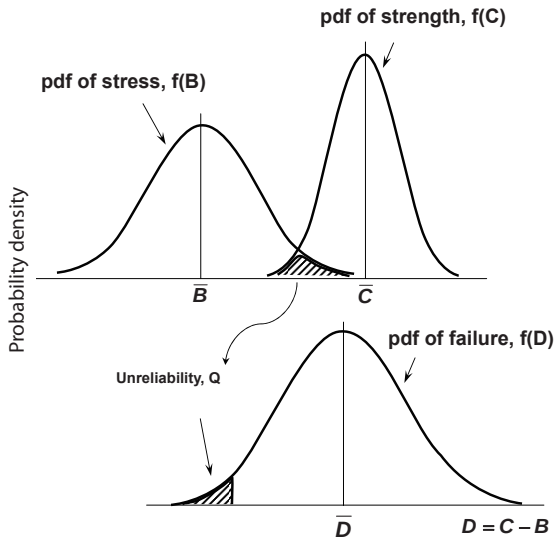

Fig. 4. The stress-strength model.

Fig. 5. Representation of major variables with the same unit.

the brackets { } indicate the set consisting of the force difference F_2-F_1. This is possible by changing the viewpoint of time from continuous to discrete because there are infinite combinations of F_2-F_1 with time as can be seen in Fig. 3. The operators of "min" and "max" denote the minimum and maximum value in the sets, respectively. The U is the minimum value of F_2-F_1 and the W is the maximum value of F_2-F_1. The fastening pins must not be cut off at the limit U for preventing the premature separation; whereas, they must be cut off at the limit W for the separation because there is no cutting force greater than the limit. The V is the value of the shearing force of the pins, which must be placed between the U and W for successful function without failures. In the present work, the V was determined to have a bias value closer to U, not a center between U and W, to give more weight to failure mode 1 than to failure mode 2.

The two failure modes can be modeled into the form of Eq. (1) by using the definition of Eq. (5) as shown below:

1) Failure mode 1 (no separation of the ejector) occurs when V>W:

$$\begin{aligned} D_1 &= C_1 - B_1 < 0 \\ &= W - V < 0 \\ &= \max\{F_2 - F_1\} - F_{\text{pin}} < 0 \end{aligned} \tag{6}$$

2) Failure mode 2 (insufficient ejection velocity) appears when V<U:

$$\begin{aligned} D_2 &= C_2 - B_2 < 0 \\ &= V - U < 0 \\ &= F_{\text{pin}} - \min_{v > v_g}\{F_2 - F_1\} < 0 \end{aligned} \tag{7}$$

The subscripts of 1 and 2 of D, C, and B in the above equations indicate the relevant failure modes. In a deterministic design method, a safety factor is generally defined as SF = $\frac{C}{B}$. According to this definition, the safety factors for failure mode 1 and failure mode 2 were calculated as 1.22 and 1.17, respectively. It is important to note, however, that they give no information about the reliability.

In the models above, the variable B_1 for failure mode 1 is identical to the variable C_2 for failure mode 2, which are a function of the F_{pin}. Similarly, C_1 is equal to B_2, which are a function of F_1 and F_2, as given in Eq. (8):

$$\begin{aligned} B_1 &= C_2 = f\{F_{\text{pin}}\} \\ C_1 &= B_2 = f\{F_1, F_2\} \end{aligned} \tag{8}$$

Eventually, the major design variables determining the ejector's reliability are summarized: F_{pin}, F_1, and F_2. Of course, each of these variables is a function of more than one variable as shown below:

$$F_{pin} = \sigma_{shear} A_{pin} \tag{9}$$

$$F_1 = C_F P_1 A_t \tag{10}$$

$$F_2 = P_2 A_{\text{cylinder}} \tag{11}$$

In Eq. (10), the thrust coefficient C_F is given (Sutton, 1992) as

$$C_F = \sqrt{\frac{2\gamma^2}{\gamma-1}\left(\frac{2}{\gamma+1}\right)^{\frac{\gamma+1}{\gamma-1}}\left[1-\left(\frac{P_e}{P_1}\right)^{\frac{\gamma-1}{\gamma}}\right]} + \frac{P_e - P_a}{P_1}\frac{A_e}{A_t} \tag{12}$$

The F_{pin} in Eq. (9) can be simply obtained by shear test in a simulated condition using the real pins. The F_1 and F_2 in Eqs. (10) and (11) can also be obtained either by direct measurement through ground-firing tests of the manufactured ejector or by calculation of multiplying the area by P_1 or P_2 measured from the tests. However, due to the lack of the number of the ejector available for the test, it would be difficult, realistically, to obtain these data sufficient to construct the *pdfs*, particularly with statistical significance. It is therefore preferable to obtain the P_1 and P_2 by calculation rather than by firing tests. Because of this, an internal ballistics model is required.

3.4 Internal ballistic model

In terms of the physical model shown in Fig. 1, we can write the mass and energy conservation equations for each chamber by assuming that all flow variables are uniform inside each chamber and the combustion gas behaves as an ideal gas.

The conservation equations for chamber 1 are:

$$\frac{d(\rho_1 V_1)}{dt} = \dot{m}_{gen} - \dot{m}_{10} - \dot{m}_{12} \tag{13}$$

$$\frac{d(\rho_1 V_1 c_v T_1)}{dt} = \dot{m}_{gen} c_p T_f - (\dot{m}_{10} + \dot{m}_{12}) c_p T_1 \tag{14}$$

$$P_1 = \rho_1 R_g T_1 \tag{15}$$

The conservation equations for chamber 2 are:

$$\frac{d(\rho_2 V_2)}{dt} = \dot{m}_{12} \tag{16}$$

$$\frac{d(\rho_2 V_2 c_v T_2)}{dt} = \dot{m}_{12} c_p T_1 - \dot{Q}_{loss} \tag{17}$$

$$P_2 = \rho_2 R_g T_2 \tag{18}$$

In the equations above, the mass flow rate generated by burning a solid propellant, $\dot{m}_{\text{gen}}$, is evaluated by

$$\dot{m}_{gen} = \rho_p A_b r_b \tag{19}$$

Here, the burning rate r_b is expressed as an exponential function of the pressure of chamber 1,

$$r_b = aP_1^n \tag{20}$$

The burning area A_b is a function of the burning distance, e, and can be obtained using the geometrical relationship of the propellant grain shape by following a normal burning law. Since the volume of chamber 1, V_1, is initially occupied by a propellant grain, it increases as the propellant burns. Thus, the volume variation should be included in the governing equations.

$$\frac{dV_1}{dt} = A_b r_b \tag{21}$$

In order to terminate the combustion of the propellant, we need to determine the burning distance with time by the following equation. When e equals web_{max}, the combustion is terminated.

$$\frac{de}{dt} = r_b \tag{22}$$

The mass flow rate flowing out of chamber 1 to the atmosphere through a nozzle, $\dot{m}_{10}$, is evaluated by assuming that the nozzle flow is always choked.

$$\dot{m}_{10} = C_D P_1 A_t \tag{23}$$

Here, the discharge coefficient, C_D, is calculated by the following expression

$$C_D = \sqrt{\gamma \left(\frac{2}{\gamma+1}\right)^{\frac{\gamma+1}{\gamma-1}} \frac{1}{R_g} \frac{M_w}{T_1}} \tag{24}$$

The mass flow rate flowing out of chamber 1 to chamber 2 through the orifices, $\dot{m}_{12}$, is dependent upon the pressures in chambers 1 and 2: If the pressure ratio of P_2 / P_1 is less than a critical pressure ratio $P_{critical} = \left(\frac{2}{\gamma+1}\right)^{\frac{\gamma}{\gamma-1}}$, the flow is choked; on the other hand, if the pressure ratio of P_2 / P_1 is greater than the critical pressure ratio, the flow is unchoked . Hence, $\dot{m}_{12}$ can be evaluated by the following expression

$$\dot{m}_{12} = \begin{cases} C_D P_1 A_{orifice}, & \text{if } \frac{P_2}{P_1} < P_{critical} \\ A_{orifice}\sqrt{\frac{2\gamma}{\gamma-1} P_1 \rho_1 \left[\left(\frac{P_2}{P_1}\right)^{\frac{2}{\gamma}} - \left(\frac{P_2}{P_1}\right)^{\frac{\gamma+1}{\gamma}}\right]}, & \text{otherwise} \end{cases} \tag{25}$$

The $\dot{Q}_{loss}$ in Eq. (17) is the heat loss of chamber 2 and cannot be neglected because the wet area of chamber 2 is considerably large compared to the small amount of hot gas flowing through the orifices. This is very difficult to evaluate theoretically and, thus, is empirically determined.

Now we have established the governing equations to evaluate P_1 and P_2. We need to solve these equations simultaneously. First, we convert these equations into forms that are easy to handle. After some mathematical manipulations, we can obtain the following six ordinary differential equations (ODE) for chambers 1 and 2.

$$\frac{d\rho_1}{dt} = \frac{\dot{m}_{gen} - \dot{m}_{10} - \dot{m}_{12} - \rho_p A_b r_b}{V_1} \tag{26}$$

$$\frac{dP_1}{dt} = \frac{\gamma R T_f \dot{m}_{gen} - \gamma R T_1 \left(\dot{m}_{10} + \dot{m}_{12}\right) - P_1 A_b r_b}{V_1} \tag{27}$$

$$\frac{dV_1}{dt} = A_b r_b \tag{28}$$

$$\frac{de}{dt} = r_b \tag{29}$$

$$\frac{d\rho_2}{dt} = \frac{\dot{m}_{12}}{V_2} \tag{30}$$

$$\frac{dP_2}{dt} = \frac{\gamma R T \dot{m}_{12} - \dot{Q}_{loss}}{V_2} \tag{31}$$

These ODEs can be solved by the Runge-Kutta integration scheme.

3.5 Monte Carlo method

In order to predict reliability according to the models of Eqs. (6) and (7) based on the probabilistic design method, the probabilistic information on the variables of C and B (in detail F_{pin}, F_1, and F_2) is necessary, including the distribution shape and its parameters such as mean and standard deviation. Basically, the *pdf* information can be obtained from many test data. However, the number of test samples is usually not sufficient to determine the *pdf* information of a certain variable. The adoption of a MC method can solve this problem. The MC method provides the *pdf* information on variables by a repeated random sampling on the computer (Rubinstein, 1981). The method also makes it possible to obtain the *pdf* of the variables which are difficult to obtain directly from the experiment by substituting the values of other variables into the associated equations. To do this, of course, information on the *pdf* of each of the variables is needed. The detailed procedure of the method consists of the following steps:

1) Generate values of the design variables consisting of the forces of C and B according to their respective distributions

2) Calculate the values of the forces of C and B using the randomly generated values of the variables
3) Calculate the value of the force D from the forces of C and B
4) Repeat steps 1 to 3 n times to obtain the pdf of D

Consequently, the reliability of failure modes can be calculated from the *pdf* of D.

4. Results

4.1 Verification of internal ballistics calculation

It is necessary to verify the internal ballistics model since the present work is based on the calculated result of P_1 and P_2 instead of the result of the ground-firing test of the ejector per se. Figure 6 represents a comparison between the firing-test result and the deterministically calculated result using the internal ballistics model at +20℃. The correction factors, which for convenience were not shown in the governing equations, were used for better fitting of the results of the experiment and calculation. Agreement in the major performance by the calculation and experiment was relatively good, which gives validity to the present internal ballistics model.

4.2 Simulation input and run

The MC simulation was carried out at the temperatures of -40℃, +20℃, and +60℃ to predict the reliability of each failure mode and to identify the most important design variables on reliability. Each simulation consists of n = 10,000 trials to obtain the *pdf* of the failure variable D of each failure mode. In each trail, the U in Eq. (3) is determined as ΔF at the time point when the impulse, by time integration of thrust F_1, reaches the level equivalent to the required velocity. The W is obtained as a maximum of ΔF by checking the value in every time increment. The V is randomly sampled in the specified distribution, based on the shear test of the pins. All the design variables and their respective distributions used in the simulation are listed in Table 1.

The *pdf* information on these variables was obtained by specimen-based tests, dimensional measurements or specified tolerances of the components. Some design variables in Table 1 were assumed as a normal distribution although a considerable number of tests were conducted. As can be seen in Fig. 7, for example, the distribution of F_{pin} obtained from the specimen tests did not comply with any of theoretical distributions. This is considered because of insufficient sample size.

4.3 Reliability prediction

Table 1. Input variables treated as a random variable in the simulation

Variable	Distribution	Remarks
Force for shearing the pins	Normal (assumed)	Shear tested
Propellant burning rate	Normal (assumed)	Measured
Propellant density	Normal (assumed)	Measured
Dimension of propellant grains	Normal	Measured
Nozzle dimension	Uniform	Given by tolerance
Separation cylinder dimension	Normal	Measured
Orifice dimension	Uniform	Given by tolerance

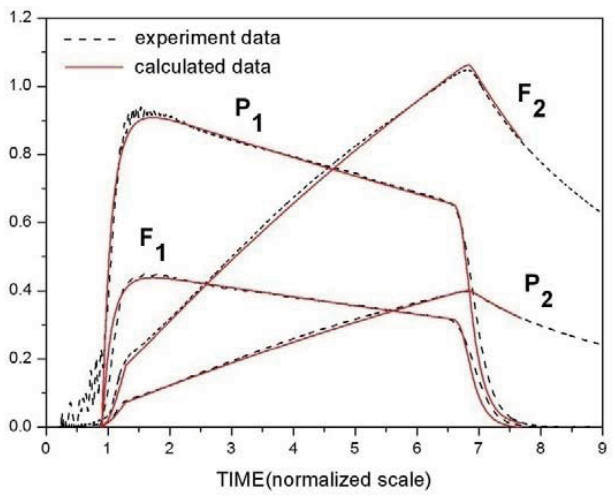

Fig. 6. Comparison of the internal ballistics performance by calculation and experiment.

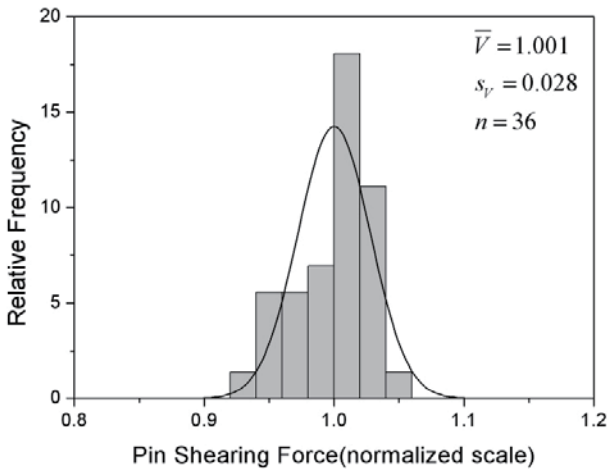

Fig. 7. Frequency distribution of the shearing force of the pins obtained from the shear test.

Figure 8 represents the frequency distributions of the variables of U, V, and W obtained from the simulation at a condition of +20℃. Those at -40℃ and +60℃ were not presented here since they were similar to that of +20℃.

The frequency distribution of each variable showed a good fit with a normal distribution function (solid line). It was observed that the distribution width of V was narrow whereas those of U and W were relatively broad. This was attributed to the difference of the variance extent and the number of design variables consisting of each variable. For example, while V depends only on the diameter and the material strength of the fastening pins with a small variance, U and W are affected by many variables such as nozzle throat size, propellant grain dimension, and propellant burning rate with a large variance. The overlapped region of the distributions of V and W, corresponding to failure mode 1, was smaller than that of V and U, equivalent to failure mode 2. These regions can be expressed in another form of failure variable D as shown in Fig. 9.

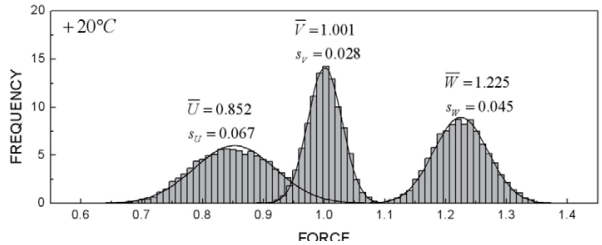

Fig. 8. Frequency distributions of each variable at 20℃.

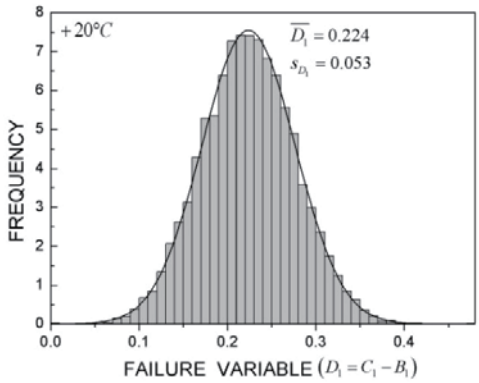

(a) Failure mode 1

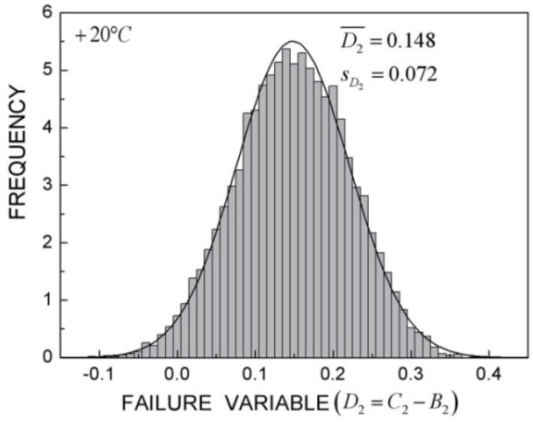

(b) Failure mode 2

Fig. 9. Distribution of the failure variable at 20℃ for (a) failure mode 1 and (b) failure mode 2.

It was also shown that D_1 and D_2 conform to the normal distribution. Because Eq. (4) is based on the assumption of a normal distribution, this consistency gives the validity of reliability prediction in the present work. According to Eq. (3), the position of zero at the *pdf* of D determines reliability. In the case of D_1, where the position of zero was relatively distant from the center of the distribution toward the left-tail, R_1 was about 99.999% at +20℃. On the contrary, in the case of D_2, where the position of zero was closer toward the center of the distribution than that of D_1, R_2 was relatively low at 97.991%. The overall reliability R_t was obtained as 97.989% by the multiplication of R_1 and R_2. This reliability value was considered rather low.

The reliability can be improved up to 99.7% by moving the mean value of V toward W (reducing the weight of failure mode 1) in the design (Fig. 10). This operation, however, is accompanied by the decreasing of the reliability of failure mode 1 having more importance. Figure 10 represents the calculation result showing the effect of the mean of V (i.e., F_{pin}) on reliability. This calculation was performed whereby the values of $Z_0=-\frac{\overline{D}}{s_D}$, varying with the mean value of V, were substituted into Eq. (4) while the standard deviations of the three variables (U, V, and W) and the means of U and W

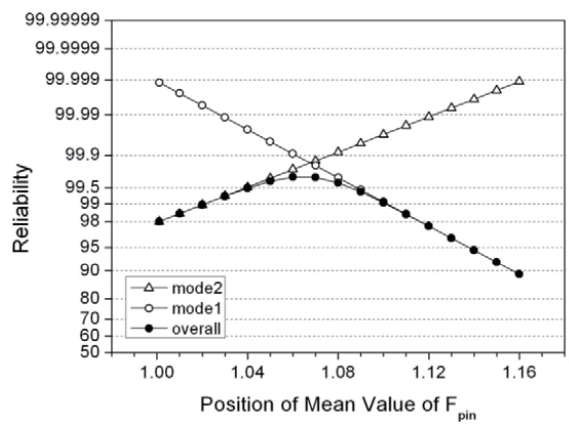

Fig. 10. The dependence of the reliability of each failure mode varied with the mean value of F_{pin}.

were fixed. As found in Fig. 10, a strong dependence of the mean value of F_{pin} on reliability implies that the strength and diameter of the pins were the most important variables of the ejector.

Figure 11 shows the dependence of reliability on the temperature. With increasing temperature, the reliability of failure mode 2 increased from 96.3% to 99.2%, whereas that of failure mode 1 did not change significantly. This is because of a change at the mean value of U (Table 2). That is, as the temperature increased, the mean value of U moved too far from that of V such that the overlapped region of these two distributions was reduced, resulting in a reliability increase for failure mode 2. The reason why the change at the mean value of U occurs can be ascribed to the fact that the greater impulse is transmitted to the missile prior to separation, due to a higher burn rate of propellant at the higher temperature. It is interesting to note that the mean values of V and W and the standard deviations of all the variables remained almost unchanged regardless of temperature.

4.4 Sensitivity analysis

To determine which variables affect reliability most significantly, the sensitivity of each design variable on reliability was analyzed. For this, the simulation was conducted under a condition of changing only one variable at a time. The change was given whereby, while the mean of a variable remained the same, the standard deviation of the variable was increased to twice that of the reference. In the case whereby the variable is the dimension of a nozzle or an orifice, the dimensional tolerance given in the design was increased instead of the standard deviation. Figure 12 summarizes the simulation result for the impact of each variable on reliability.

As indicated in Fig. 12, the three design variables play an important role in the reliability of both failure modes: the separation cylinder diameter, orifices size, and the pin strength. An increase of the variance of the first two variables caused a noticeable decrease in both reliabilities. This is because the variation of ΔF becomes large by increasing the variance of the variables. In other words, an excessively large orifice or separation cylinder makes large such that the possibility of the premature separation increases; on the contrary, an excessively small orifice or separation cylinder gives a high chance of failure in cutting the pins, resulting in a separation failure. Similarly, the variance of the latter variable, depending on the diameter and material strength of the pins, also had a significant influence on reliability since excessively high or low pin strength increases the failure possibility in both modes. Therefore, the variance as well as the mean of the diameter and material strength of pins should also be precisely controlled for high reliability. Contrary to our expectation, however, the propellant grain size and the nozzle throat size have less influence on reliability in both of the failure modes. Through this analysis, one can identify important variables and thus give priority to the variables for controlling the dimension and tolerance of the each component in design or in fabrication processes.

Table 2. Temperature effects on the distribution parameters of U, V, and W

	U		V		W	
Temperature, ℃	$\bar{U}$	s_u	$\bar{V}$	s_v	$\bar{W}$	s_W
-40	0.875	0.065	1.000	0.028	1.220	0.042
+20	0.852	0.067	1.001	0.028	1.225	0.045
+60	0.830	0.066	1.000	0.028	1.221	0.045

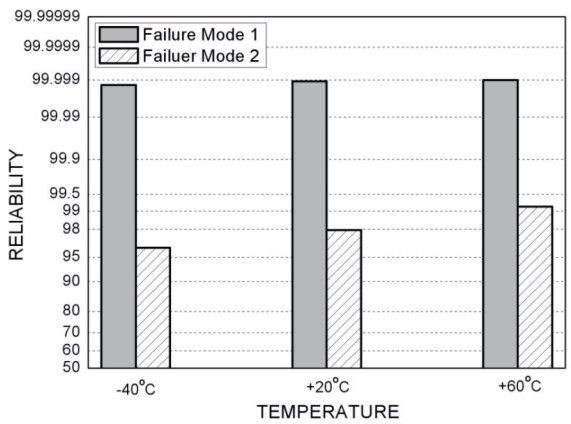

Fig. 11. Reliabilities of the failure modes at various temperatures.

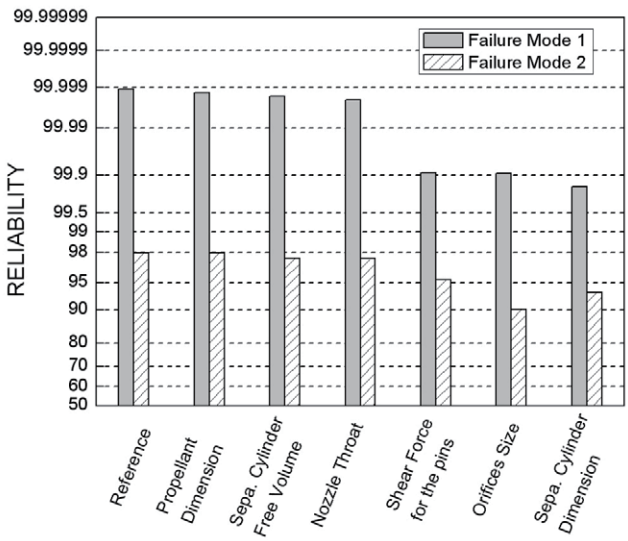

Fig. 12. The effects of the variance of the design variables on reliability.

5. Conclusions

In the present work, a particular separation mechanism of the newly devised self-separable ejector is introduced for man-portable missiles. Due to a limited number of items available to test, reliability evaluation on major functions of the ejector such as ejection and separation has become a challenging problem. In this respect, the methodology is presented based on a probabilistic design method to predict reliability without numerous firing tests. This method can not only provide advantage in respect of a schedule to correct problems in the design as well as in fabrication processes because it can be applicable to all program phases, but also gives information on important variables in performance. From the simulation result, the following conclusions were drawn:

1. It was found that the strength and diameter of the fastening pins were the most influencing variables on reliability. The sensitivity analysis result also revealed that the orifices' size and separation-cylinder's diameter have a considerable influence on reliability of both ejection and separation.

2. The internal ballistics model developed for calculating the performance of the ejector was in good agreement between the firing test results and the calculation results, which gives validity to the present work.

References

Johnson, R. A. (1988). Stress-strength models for reliability. In P. R. Krishnaiah and C. R. Rao, eds. *Handbook of Statistics, Vol 7: Quality Control and Reliability*. Amsterdam: North-Holland. pp. 27-54.

Kececioglu, D. (2003). *Robust Engineering Design-by-Reliability with Emphasis on Mechanical Components & Structural Reliability, Vol. 1*. Lancaster: DEStech Publications. pp. 1-67.

Perkins, D. and Fragola, J. (1989). Propulsion reliability-an historical perspective. *Proceedings of the 25th AIAA/ASME/SAE/ASEE Joint Propulsion Conference*, Monterey, CA. AIAA-1989-2623.

Rubinstein, R. Y. (1981). *Simulation and the Monte Carlo Method*. New York: Wiley. pp. 114-157.

Sutton, G. P. (1992). *Rocket Propulsion Elements: An Introduction to the Engineering of Rockets*. 6th ed. New York: Wiley. p. 59.

Wood, B. B. (1983). *Bayesian Reliability Test Plans for One-Shot Devices [USAFA TR-84-01]*. US Air Force Academy.

Zhang, W. and Shiue, W. K. (2001). General reliability test plans for one-shot devices. In H. Pham, ed. *Recent Advances in Reliability and Quality Engineering*. Singapore: World Scientific. pp. 51-60.